American Mineralogist, Volume 82, pages 923–930, 1997

Intersite partitioning of Mg and Fe in Ca-free high-pressure *C*2/*c* clinopyroxene

A.B. WOODLAND,[1] C. MCCAMMON,[2] AND R.J. ANGEL[2]

[1]Mineralogisches Institut, Universität Heidelberg, Im Neuenheimer Feld 236, D-69120 Heidelberg, Germany
[2]Bayerisches Geoinsitut, Universität Bayreuth, D-95440 Bayreuth, Germany

ABSTRACT

The intracrystalline distribution of Mg and Fe^{2+} on the M1 and M2 octahedral sites in high-*P C*2/*c* $(Mg,Fe)SiO_3$ clinopyroxene has been determined on quenched samples using ^{57}Fe Mössbauer spectroscopy. Although the recovered samples that were measured had the low-*P* ($P2_1/c$) structure, the ordering state of the high-*P* polymorph is believed to have been preserved because the high-*P* *C*2/*c* → low-*P* $P2_1/c$ transformation occurred at room temperature during the final stages of decompression of the experiments. Under such conditions significant cation diffusion is unlikely. Low temperature (81 K) Mössbauer spectra indicate that Fe^{2+} is strongly ordered onto the M2 sites, with an average K_D Å 4.0(8) for the intersite exchange reaction:

$$Fe^{2+}(M1) + Mg^{2+}(M2) = Fe^{2+}(M2) + Mg^{2+}(M1) \quad (1)$$

Because the samples were quenched from high temperature (1200–1275 °C) at 9.5 GPa, the temperature to which the measured ordering state corresponds remains problematic. However, a sample re-annealed at 1000 °C is more ordered than the original sample synthesized at 1275 °C, suggesting that high-temperature cation distributions in high-*P* clinopyroxene can be quenched in the multi-anvil experiments. Therefore, we conclude that the measured cation distributions correspond approximately to the conditions of the experiments. A small compositional dependence of cation ordering also exists, indicating subregular behavior across the binary join. A fit to the data yields $\Delta G^{o}_{exch} = -11.9$ (2.0) kJ/mol at 1275 °C for the exchange Reaction 1, which describes the ordering behavior on the octahedral sites in the clinopyroxenes.

Comparison with data for orthopyroxene, which were obtained mostly at 1 atm, indicates that the state of ordering in orthopyroxene and high-*P* clinopyroxene is similar, especially if cation ordering in the high-*P* clinopyroxene has a small pressure dependence. The similarities are consistent with the observed structural similarities between the two polymorphs.

INTRODUCTION

Ca-poor ferromagnesian pyroxene is an important constituent in the Earth's upper mantle. Although such pyroxene is usually considered to have an orthorhombic structure, recent experimental studies demonstrated that a monoclinic polymorph with the *C*2/*c* structure is stable at high pressures and modest temperatures for both the enstatite ($MgSiO_3$) and ferrosilite ($FeSiO_3$) end-member compositions (Angel et al. 1992; Hugh-Jones et al. 1994). It is, therefore, likely that $(Mg,Fe)SiO_3$ solid solutions also undergo this orthorhombic-to-monoclinic transformation at high pressure, implying that the monoclinic phase could exist in parts of the Earth's mantle. Woodland and Angel (1997) have suggested that, for a typical mantle pyroxene composition of $X_{En} = 0.9$, the monoclinic *C*2/*c* polymorph becomes stable at depths of about 300 km. Considering that pyroxene is progressively incorporated into the garnet structure with increasing pressure, it is likely that the existence of high-*P* ferromagnesian clinopyroxene is limited to an ~ 200 km thick zone straddling the 400 km discontinuity (Woodland and Angel 1997). Therefore, the construction of viable mineralogical models of the Earth's upper mantle and transition zone requires consideration of the thermodynamic properties of high-*P* *C*2/*c* ferromagnesian clinopyroxene.

The intracrystalline distribution of Mg and Fe^{2+} on the crystallographically non-equivalent M1 and M2 octahedral sites in the structure is of particular interest because of its effect on the excess thermodynamic properties of the clinopyroxene solid solutions. An obvious question is whether or not the intersite partitioning of Mg and Fe^{2+} is different from that in orthopyroxene. To address these points we synthesized clinopyroxene solid solutions along the $MgSiO_3$-$FeSiO_3$ join and then used ^{57}Fe Mössbauer spectroscopy to determine the relative distribution of Fe^{2+} on the M1 and M2 sites. This approach was previously applied successfully to orthopyroxene solid solutions (e.g., Virgo and Hafner 1969; Skogby et al. 1992; Do-

0003–004X/97/0910–0923$05.00

TABLE 1. Experimental results

Sample	Temperature (°C)	Pressure (GPa)	Duration (hr)	X_{Fs}* (probe)	%M1†	X_{Fe}^{M1}‡	X_{Fe}^{M2}‡	K_D‡
U-1037	1200	9.7	12.0	0.108(24)	0.306(21)	0.066(15)	0.150(34)	2.5(8)
H-277b	1275	9.5	11.7	0.296(31)	0.292(10)	0.173(19)	0.419(44)	3.5(5)
H-162	1275	9.5	12.5	0.387(16)	0.308(5)	0.238(13)	0.536(23)	3.7(3)
U-1056a	1275	9.5	12.5	0.597(20)	0.351(6)	0.420(18)	0.774(29)	4.8(6)
H-157	1200	9.5	12.0	0.643(30)	0.366(9)	0.470(25)	0.816(40)	5.0(1.0)
H-272	1275	9.5	11.5	0.680(18)	0.392(9)	0.533(20)	0.827(26)	4.2(6)
H-346§	1295	7.5	9.5	0.690(15)	0.404(3)	0.557(18)	0.823(23)	3.7(5)
H-275	1000	9.0	5.0	0.694(16)	0.373(7)	0.517(16)	0.871(22)	6.3(1.0)
U-1033	1200	9.0	12.0	0.711(17)	0.394(6)	0.560(20)	0.862(25)	4.9(9)
U-1056b	1275	9.5	12.5	0.800(20)	0.431(7)	0.690(24)	0.910(28)	4.6(1.4)
U-1035	1200	9.0	12.5	0.801(20)	0.439(5)	0.703(24)	0.899(28)	3.8(1.0)
H-277a	1275	9.5	11.7	0.899(10)	0.471(5)	0.847(20)	0.951(21)	3.5(1.5)
U-1258	1150	8.0	20.0	1.00	0.491(6)	0.982(20)	1.018(20)	1.0(1.6)

* Composition from microprobe analysis with estimated standard deviation.
† Relative spectral area corresponding to Fe on the M1 site with statistical error in fit. Mössbauer data collected at 81 K.
‡ Values are for Equilibrium 1. Uncertainties determined by propagation of uncertainties in composition and spectral area.
§ Used Au capsule.

meneghetti and Steffen 1992). By combining the spectroscopic results with bulk compositions measured with the microprobe, the full octahedral site occupancy can be derived for each sample. We conclude with a brief comparison of the ordering behavior of high-*P* clinopyroxene and orthopyroxene.

EXPERIMENTAL METHODS

The starting materials used for synthesizing the ferromagnesian clinopyroxene solid solutions were stoichiometric mixtures of fayalite + MgO + quartz ground together with ~6 wt% BaO-B_2O_3 (78 wt% BaO) flux. The syntheses were performed in a multi-anvil press at the Bayerisches Geoinstitut, Universität Bayreuth, using Toshiba F-grade tungsten carbide cubes with an 11 mm truncated edge. The methods follow those described in Woodland and O'Neill (1993). Mechanically sealed capsules made from 1.7 mm diameter silver-tubing were used to prevent Fe loss during the experiments (in one case gold was used, see Table 1). The experimental conditions were chosen to lie within the stability field for *C2/c* high-*P* clinopyroxene in the end-member $MgSiO_3$ system (Table 1, Fig. 1). Because Fe acts to lower the pressure of the orthorhombic to high-*P* monoclinic transition, these conditions assured that the high-*P* clinopyroxene polymorph was produced for all compositions across the $MgSiO_3$-$FeSiO_3$ join (Woodland and Angel 1997). The accuracy in pressure is estimated to be ± 0.3 GPa, and the temperature gradient across the sample is considered to be <25 °C (c.f. Canil 1994). The duration of the multi-anvil experiments was between 5 and 12.5 h with most exceeding 11 h (Table 1). The experiments were quenched at pressure and then slowly decompressed at room temperature. Because of the unquenchable nature of the high-*P C2/c* polymorph (Angel et al. 1992; Hugh-Jones et al. 1994), the recovered clinopyroxenes always had the low-*P* $P2_1/c$ structure. However, it was considered that the samples would preserve the Mg-Fe^{2+} ordering state corresponding to the high-*P C2/c* polymorph because the transformation to the $P2_1/c$ structure occurred only at room temperature and significant cation re-arrangement is unlikely under such conditions.

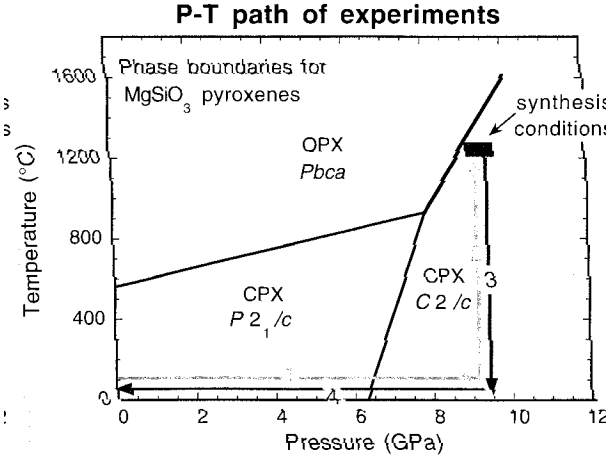

FIGURE 1. Schematic pressure-temperature path for the synthesis of $(Mg,Fe)SiO_3$ clinopyroxenes. Step 1: pressurization at room temperature; Step 2: heating to achieve the desired pressure-temperature conditions for the synthesis; Step 3: termination of experiment by shutting off power while at high pressure; Step 4: decompression to ambient conditions. The phase boundaries for $MgSiO_3$ pyroxenes are shown for reference, indicating that the experiments were within the stability field of *C2/c* clinopyroxene.

After the experiments, the compositions of the pyroxenes were determined using a Cameca SX-51 electron microprobe under the operating conditions of 15 kV and a 20 nA sample current with 20 s counting times on the peak and background. The standards used were wollastonite for Si, MgO for Mg, and Fe_2O_3 for Fe, and the raw counts were recalculated using the PAP program supplied by Cameca. The sample compositions, along with their associated standard deviations (1σ) are provided in Table 1. The samples were also analyzed by powder X-ray dif-

fraction to assure that they were monoclinic. The measured structural parameters will be reported elsewhere.

Samples for powder X-ray diffraction analysis and Mössbauer spectroscopy were prepared by gluing the ground pyroxene powder onto a thin plastic foil. Mössbauer absorber thicknesses varied from 1 to 7 mg Fe/cm^2. Mössbauer spectra were recorded in transmission mode on a constant acceleration Mössbauer spectrometer with a nominal 50 mCi ^{57}Co source in a 6 μm Rh matrix. The velocity scale was calibrated relative to 25 μm α-Fe foil using the positions certified for National Bureau of Standards standard reference material no. 1541; line widths of 0.28 mm/s for the outer lines of α-Fe were obtained at room temperature. Mössbauer spectra were recorded at low temperature (81 ± 2 K) using a continuous flow cryostat with the sample in nitrogen vapor. The spectra were analyzed using the commercially available fitting programs NORMOS (written by R.A. Brand and distributed by Wissenschaftliche Elektronik GmbH, Germany) and MOSMOD (written and distributed by D.G. Rancourt, University of Ottawa, Canada).

Determination of site occupancies

Spectra of the clinopyroxene solid solutions consist of two doublets corresponding to Fe^{2+} on the M1 and M2 octahedral sites, respectively (Fig. 2). The relative areas of these two doublets correspond to the relative abundance of Fe^{2+} on each site, and can be used to derive the octahedral site distribution of Fe^{2+}. Combining this result with the microprobe compositions, the site occupancies of Mg and Fe^{2+} can be calculated.

Visual examination of the Mössbauer spectra for (Fe,Mg)SiO_3 clinopyroxene reveals a slight asymmetry between low- and high-velocity components of the quadrupole doublets (Fig. 2). McCammon and Tennant (1996) observed a similar asymmetry in both room- and high-pressure Mössbauer spectra of $FeSiO_3$ $P2_1/c$ clinopyroxene. Statistically equivalent fits could be made to the present spectra with either unequal widths or unequal areas of the low- and high-velocity components of each quadrupole doublet. Unequal areas are most likely caused by preferred orientation; a possibility given the nature of the absorbers (powder glued onto a plastic foil). This was tested by remaking two of the absorbers. The sample was removed from the plastic foil, mixed with a large quantity of benzophenone, and placed loosely in a sample holder with no stress applied to the powder. The doublet asymmetry remained unchanged, indicating a factor other than preferred orientation. The other likely cause of asymmetric doublets is from unequal line broadening of the low- and high-velocity peaks because of variation in the local Fe^{2+} environment within the pyroxene. Such is the case for both the M1 and M2 doublets in aluminous orthopyroxenes, which is attributable to the presence of a variety of next nearest neighbor configurations about the Fe^{2+} cations, resulting in a statistical distribution of hyperfine parameters when all chemical environments are summed together (Seifert 1983). Mössbauer spectra corresponding

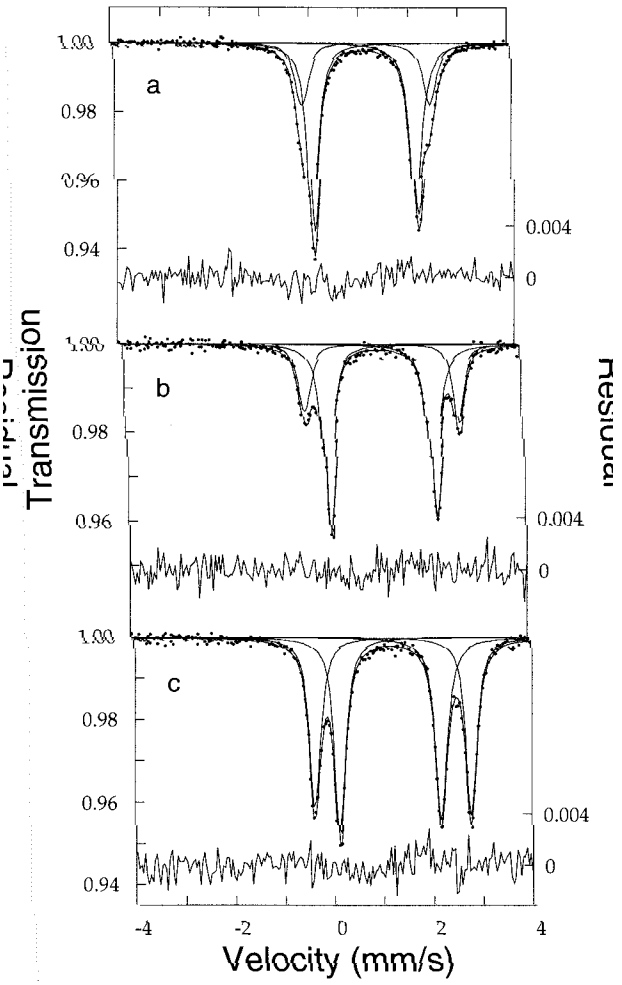

Figure 2. Mössbauer spectra of of (Mg,Fe)SiO_3 clinopyroxenes. (**a**) Room-temperature spectrum from sample H-277b with X_{Fs} = 0.296(31). (**b**) 81 K spectrum from sample H-277b. Note the improved resolution of the doublet corresponding to Fe^{2+} on the M1 site in comparison with that in **a**. (**c**) 81 K spectrum from sample H-277a with X_{Fs} = 0.899(10). The fitting procedure adopted for the spectra is described in the text.

to hyperfine parameter distributions can be modeled using sums of Voigt lineshapes (Rancourt and Ping 1991). Several models incorporating different constraints and lineshapes were tested, using the chi-squared values, consistency of parameters between samples, and convergence of the fitting process to evaluate the appropriateness of each model. The simplest model with the smallest number of adjustable parameters that could successfully fit all of the Mössbauer spectra was a fit with four Voigt singlets, where the position, Lorentzian linewidth, and Gaussian standard deviation of each singlet were allowed to vary. The areas of the high- and low-velocity components of each quadrupole doublet were constrained to be equal, as expected for a random powder absorber. The derived hyperfine parameters were the same regardless of whether a model assuming equal component areas but unequal

linewidths (the model used in the present study) or a model assuming equal component linewidths but unequal areas (McCammon and Tennant 1996) was used. The values of the center shift and quadrupole splitting determined in the present work for $FeSiO_3$ $P2_1/c$ clinopyroxene agree within experimental error with the values reported by McCammon and Tennant (1996).

Many factors influence the relationship between the measured relative areas of the doublets and the true relative atomic proportions of Fe^{2+} on the two octahedral sites (e.g., Rancourt 1989). One of the significant factors is finite sample thickness, which causes spectral distortion and leads to overestimation of the less abundant components (Fe^{2+} on the M1 site, in the case of pyroxene). Skogby et al. (1992) made a thickness correction by measuring orthopyroxene Mössbauer spectra at absorber thicknesses ranging from 1.5 to 15.5 mg Fe/cm^2 and extrapolating to zero thickness. A more rigorous approach would be (1) to deconvolute the experimental data to obtain the spectrum in the thin limit (Rancourt 1989) or (2) to fit the experimental data directly with the full transmission integral. To evaluate the influence of thickness effects on our results, we applied both computational methods to datasets from two samples with different compositions and the highest absorber thicknesses. Results from both methods agreed with each other within experimental error and indicated that the effect on the derived partition coefficient was smaller than the experimental error. Thickness effects are also known to become more significant as the area difference between spectral components increases, which occurs at low Fe concentrations in the (Fe,Mg)SiO_3 pyroxene solid solutions (Rancourt 1989). However, the absorber thicknesses also tend to be lower in this compositional range because of the limited amount of material available from the high-pressure syntheses, thus compensating for the thickness effects. Because the influence of thickness effects is smaller than the experimental error, we have not applied a thickness correction.

Another important factor in calculating site occupancies is consideration of the recoil-free fractions because a significant difference between recoil-free fractions for Fe^{2+} occupying the M1 and M2 sites changes the relative areas of the subspectra. The relative site populations are given by

$$\frac{n_i}{n_{\text{total}}} = \frac{\overline{f}}{f_i}\frac{A_i}{A_{\text{total}}}$$

where n_{total} and n_i are the total number of Fe atoms and the number of Fe atoms on the site i, respectively, A is the spectrum area (A_{total} is the total area and A_i is the subspectral area corresponding to the i^{th} site) and f_i is the recoil-free fraction on the i^{th} site and $\overline{f}$ is the average recoil-free fraction given by

$$\overline{f} = \frac{1}{n_{\text{total}}}\sum_i n_i f_i$$

(e.g., Rancourt et al. 1994). As no data are currently available for recoil-free fractions in Ca-free clinopyroxenes, the present data were used to assess the effect of differing recoil-free fractions. Using the Debye model and the center shift data at 293 and 81 K, the recoil-free fractions were calculated for Fe^{2+} occupying the M1 and M2 sites for each sample composition from the temperature dependence of the second-order Doppler shift (see McCammon et al. 1995 for a description of the procedure). The results indicate that recoil-free fractions for Fe^{2+} occupying the M1 and M2 sites are equal within experimental error for all sample compositions (see next paragraph, however). An independent test of this conclusion can be made by examining the relative area data. When recoil-free fractions are equal for Fe^{2+} on both sites, the corresponding subspectra areas should be temperature independent. Fitting both the 293 and 81 K Mössbauer data to the same model yielded the same subspectra area ratios within experimental error in all cases. We conclude, therefore, that no correction for differing recoil-free fractions is required.

The intracrystalline partition coefficient for each composition was determined from only the low-temperature Mössbauer data because the improved resolution of spectral components (compare Figs. 2a and 2b) reduces the experimental error. The low temperature also reduces the effect from differing recoil-free fractions. (There appears to be a slight systematic difference between the recoil-free fractions for Fe^{2+} on the M1 and M2 sites for bulk compositions close to the Mg end-member. However, the large experimental error—only two data points were available to calculate the recoil-free fractions at each composition—precludes an evaluation of whether this difference is significant.)

Uncertainties in the partition coefficients were assessed by propagating the uncertainties in both the composition and the determination of the relative areas of the Mössbauer subspectra. The sensitivity of the partition coefficient to these uncertainties varies significantly with bulk composition. Near the Fe end-member, where the site occupancies are nearly identical, a small change in site occupancy produces a large change in K_D; whereas close to the Mg end-member K_D is not nearly so sensitive. Although the absolute error in determining the M1 and M2 site occupancies is roughly the same across the solid solution series, the effect on K_D is quite different. Near the Mg end-member ($X_{Fe} = 0.3$) an uncertainty of ± 1 mol% in composition or a ± 1% absolute error in the M1 relative area produces a 4% relative error in the partition coefficient, whereas near the Fe end-member, ($X_{Fe} = 0.9$) the same $\pm$ 1% uncertainties in composition and area ratio result in relative errors of 22 and 38%, respectively. The calculated partition coefficients are sensitive to the type of model (symmetric or asymmetric) used to fit the Mössbauer spectra. However, a symmetric spectral model was judged inappropriate on the basis of the significantly higher χ^2 values (an increase in χ^2 of > 15%) and the consistently larger residuals that indicated a real asymmetry between the component doublets. In any case, we

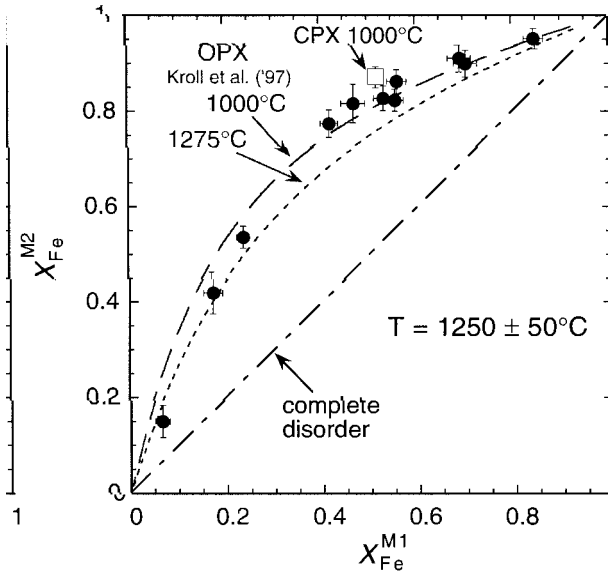

FIGURE 3. Rooseboom plot of site occupancies of Fe^{2+} between the M1 and M2 sites. The closed circles are samples synthesized at 1200–1295 °C. The open square is a sample re-annealled at 1000 °C. If the Fe^{2+} distribution were completely disordered, the data points would fall on the dashed diagonal line. A strong preference for Fe^{2+} to occupy the M2 sites is indicated by the data. For reference, the recent model of Kroll et al. (1997) for Mg-Fe orthopyroxenes is also provided, showing their 1000 °C and 1275 °C isotherms.

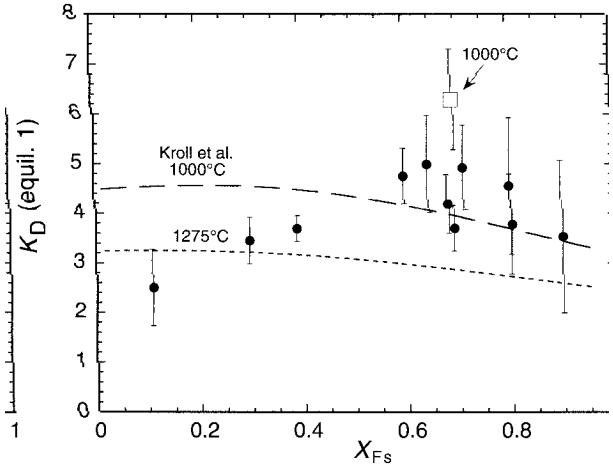

FIGURE 4. K_D for the Mg-Fe exchange Equilibrium 1 plotted as a function of ferrosilite content in the clinopyroxenes. The dashed curves are the 1000 °C and 1275 °C isotherms from the model of Kroll et al. (1997) for Mg-Fe orthopyroxenes.

note that within a particular type of spectral model (symmetric or asymmetric), partition coefficients are less sensitive to details such as line shape (Lorentzian or Voigt) and interspectrum constraints (e.g., whether all Voigt lines have the same Lorentzian line width).

RESULTS

At the conditions most experiments were performed, 9.0–9.7 GPa and 1200 or 1275 °C, solid solution was found to be complete across the $MgSiO_3$-$FeSiO_3$ join. In addition, no Fe^{3+} was detectable in the Mössbauer spectra from any of the samples, indicating that the clinopyroxenes are true binary solid solutions.

The Fe^{2+} site occupancies of the clinopyroxene solid solutions are best viewed in a Rooseboom plot (Fig. 3). If Fe^{2+} showed no site preference (i.e., complete disorder), the data points would fall on the dashed diagonal line in Figure 3. This is clearly not the case, with Fe^{2+} being strongly ordered onto the M2 sites. Thermodynamically, the partitioning of Fe^{2+} and Mg between the M1 and M2 sites can be considered in terms of the exchange reaction:

$$Fe^{2+}(M1) + Mg^{2+}(M2) = Fe^{2+}(M2) + Mg^{2+}(M1) \quad (1)$$

with K_D defined as:

$$K_D = \frac{X^{M2}_{Fe} X^{M1}_{Mg}}{X^{M1}_{Fe} X^{M2}_{Mg}}$$

An average K_D of 4.0(8) (n = 11) is obtained from the clinopyroxenes synthesized between 1200 and 1295 °C (Table 1). A slight compositional dependence is apparent when K_D is plotted against the ferrosilite content, with K_D slowly increasing with bulk Fe content (Fig. 4). As such, this average value for K_D should only be considered to be approximate. The most Fe-rich sample (X_{Fs} = 0.899) deviates from this trend. However, considering the large uncertainty in the K_D for this and the neighboring samples, the significance of this anomalous behavior is unclear (Fig. 4).

Because the intersite partitioning of cations is a thermally activated process (e.g., Ganguly 1982), interpretations of the partitioning data must consider the temperature at which a particular ordering state was frozen. The kinetics of re-ordering in analagous orthopyroxene solid solutions has been shown to be so rapid that equilibrium ordering states above 900 °C are unquenchable (Anovitz et al. 1988). With respect to our high-P clinopyroxenes synthesized at 1200 °C, the question then arises: Does the observed cation distribution truly correspond to the temperature of the experiment or has partial re-ordering occurred during the quench? In an attempt to address this question we re-annealed part of an Fe-rich clinopyroxene sample at 1000 °C that was previously synthesized at 1275 °C (experiments H-275 and H-272, respectively, Table 1). The re-annealed sample has a K_D = 6.3(1.0), which is significantly more ordered than the K_D = 4.2(6) obtained for the original, higher temperature sample (Fig. 5). This suggests that high-temperature cation distributions in high-P clinopyroxene can be quenched in our multi-anvil experiments and that the measured cation distributions reported here correspond approximately to the conditions of the experiments. That a small degree of re-ordering occurred during the quench in one or both samples remains a possibility, as accurate in situ measure-

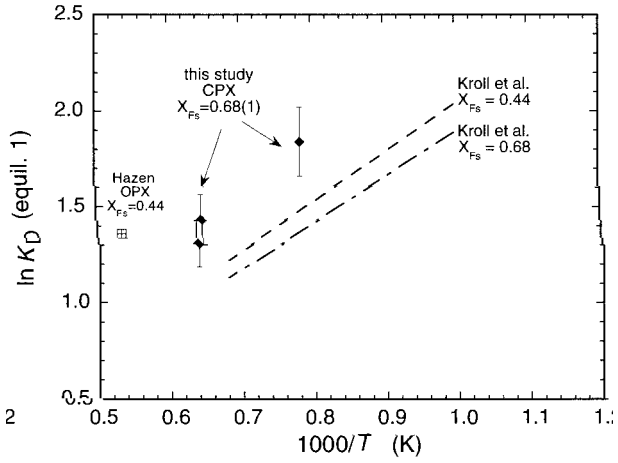

FIGURE 5. In K_D for exchange Equilibrium 1 vs. $1/T$ (K) for clinopyroxenes with $X_{Fs} = 0.68(1)$. Note the difference in K_D between 1275 °C and 1000 °C, implying that high-temperature ordering states can be preserved in high-pressure experiments in the multi-anvil press. Shown for reference are the model values of Kroll et al. (1997) for orthopyroxene with $X_{Fs} = 0.68$ and 0.44. An orthopyroxene synthesized by Hazen et al. (1993) at high pressure and temperature is also plotted, further suggesting that ordering states corresponding to temperatures in excess of 1000 °C can be preserved in multi-anvil experiments.

ments are not currently feasible. However, if the rates of ordering were as rapid as that reported by Anovitz et al. (1988) for orthopyroxene at 1 atm, then both clinopyroxene samples should have yielded the same K_D. This is clearly not the case (Fig. 5). The kinetics of cation ordering could also be compositionally dependent, as appears to be the case for orthopyroxene, where ordering is reported to be more rapid in Fe-rich compositions (e.g., Anovitz et al. 1988; Sykes-Nord and Molin 1993). In this context the observed small increase in K_D with increasing ferrosilite content in the high-*P* clinopyroxenes (Figs. 3 and 4) could be attributed to the ''freezing-in'' of ordering states representing progressively lower temperatures, as the rates of ordering become faster. However, the fact that different ordering states can be preserved in Fe-rich ($X_{Fs} = 0.69$) samples annealed at different temperatures makes this possibility unlikely (see above). In addition, the sample richest in Fe (H-277a) should then be the most ordered sample, which is not the case (Table 1). The preservation of high-temperature ordering states in our experiments could be related to an extremely rapid quench rate of the small sample masses in the multi-anvil press or to an effect of high pressure, slowing the intersite exchange of cations.

Describing the energetics of cation ordering in Mg-Fe clinopyroxene not only involves the exchange Reaction 1, but also the reciprocal ordering reaction (e.g., Sack 1980):

$$Mg_2Si_2O_6 + Fe_2Si_2O_6 = Fe(M2)Mg(M1)Si_2O_6 + Mg(M2)Fe(M1)Si_2O_6 \quad (2)$$

for which the Gibbs free energy is ΔG^{o}_{rec}. Following the development given by Thompson (1969), and more specifically for orthopyroxene solid solutions by Sack (1980), the vibrational portion of the Gibbs free energy can be expressed as a Taylor expansion in terms of two parameters, a compositional $(2X_{Fs} - 1)$ and an ordering parameter $(X^{M2}_{Fe} - X^{M1}_{Fe})$. The condition for internal equilibrium in the high-*P* clinopyroxene solid solutions results in the following expression:

$$0 = RT \ln K_D(1) + \Delta G^{o}_{exch} + (W^{M1} - W^{M2})(2X_{Fs} - 1) - (W^{M2} + W^{M1} - \Delta G^{o}_{rec})(X^{M2}_{Fe} - X^{M1}_{Fe}) \quad (3)$$

where $\Delta G^{o}_{exch} = (G^{o}_{Fe^{M2}Mg^{M1}Si_2O_6} - G^{o}_{Mg^{M2}Fe^{M1}Si_2O_6})$. Assuming that the measured K_D corresponds to the temperature of the experiments, a least-squares fit to our six data points at 1275 °C and 9.5 GPa (Table 1) yields $\Delta G^{o}_{exch} = -11.9$ (2.0) kJ/mol, $(W^{M1} - W^{M2}) = -3.5(9)$ kJ/mol and $(W^{M2} + W^{M1} - \Delta G^{o}_{rec}) = 19.7(6.6)$ kJ/mol. These results indicate that a subregular mixing model is required to describe the distribution of Mg and Fe^{2+} on the M1 and M2 sites in high-*P* clinopyroxene (i.e., $W^{M1} - W^{M2}$ is non-zero). The individual values for W^{M1}, W^{M2}, and ΔG^{o}_{rec} cannot be determined because of the lack of sufficient constraints from the available partitioning data. However, assuming that $\Delta G^{o}_{rec} = 0$, we obtain $W^{M1} = 8.1$ kJ/mol and $W^{M2} = 11.6$ kJ/mol. Derivation of the temperature dependencies of these thermodynamic parameters awaits further study.

Single-crystal X-ray structure refinement is an alternative method for extracting site occupancies. Although such refinements were also attempted, it was found that twinning usually developed from the $C2/c \rightarrow P2_1/c$ transformation that occurred upon decompression of the experiment (see above), rendering nearly all crystals unsuitable for such measurements. In only one instance (sample H-162) was it possible to obtain a reasonable refinement and extract the octahedral site occupancies. The derived $K_D = 4.5(4)$ is 1.5 combined estimated standard deviations larger than the K_D obtained from Mössbauer spectroscopy, which is a statistically insignificant difference (Table 1). Full details of the single-crystal X-ray structure refinement will be reported elsewhere.

COMPARISON WITH ORTHOPYROXENE

The intersite distribution of Fe^{2+} and Mg in orthopyroxene has been the subject of numerous studies (Virgo and Hafner 1969; Saxena and Ghose 1971; Sack 1980; Ganguly 1982; Anovitz et al. 1988; Domeneghetti et al. 1992; Shi et al. 1992; Skogby et al. 1992; Yang and Ghose 1994; Kroll et al. 1997). An assessment of the attributes of these studies is beyond the scope of this paper. However, it is interesting to compare the ordering states of our high-*P* clinopyroxene solid solutions with those observed in orthopyroxene. We have chosen the results of Kroll et al. (1997) for direct comparison because this is the most recent work currently available. Their model cation distributions and K_D measurements at 1000 and 1275 °C are provided in Figures 3–5 for comparison with the results

for the high-*P* clinopyroxenes. The following discussion is also qualitatively valid if the model of Yang and Ghose (1994) were used for comparison instead. Many studies of orthopyroxene solid solutions, including that of Kroll et al. (1997), have found K_D to be compositionally dependent. This is also the case for the high-*P* clinopyroxenes, although the functional form of the dependency is different than for orthopyroxene (Fig. 4). The anomalous ordering behavior observed for Fe-rich orthopyroxenes (i.e.,Yang and Ghose 1994; Virgo and Hafner 1969) is consistent with that observed for our most Fe-rich high-*P* clinopyroxene sample.

Comparison of the cation ordering in high-*P* clinopyroxene with that of orthopyroxene requires extrapolating the model of Kroll et al. (1997) to the temperatures of our experiments. Inspection of Figures 3 and 4 reveals that although the ordering state is similar in Mg-rich compositions, the high-*P* clinopyroxene is more ordered than orthopyroxene in Fe-rich compositions. The clinopyroxene re-annealed at 1000 °C is also observed to be more ordered than the analogous orthopyroxene (Fig. 4). This contrasting result for compositions with $X_{Fs} > 0.6$ is surprising in light of the structural similarities between the orthorhombic and *C*2/*c* monoclinic polymorphs. In fact, the M2 site in *C*2/*c* clinopyroxene is slightly less distorted than in orthopyroxene, leading to the expectation of a more disordered state in *C*2/*c* clinopyroxene because the M2 and M1 sites are structurally more similar to one another (Hugh-Jones et al. 1995). One possible explanation is that a small pressure effect on cation ordering exists, as Hazen and Navrotsky (1996) have suggested for orthopyroxene. They reported a small positive volume of disordering, $\Delta V_{disorder} = V_{disordered} - V_{ordered}$, for Mg-Fe orthopyroxenes, which would cause K_D to increase with increasing pressure. According to the relationship between molar volume and cation site occupancy derived by Domeneghetti et al. (1995) $\Delta V_{disorder}$ is a function of composition with a maximum at $X_{Fs} = 0.5$. Considering the similarities in the compression behavior of the M1 and M2 polyhedra in high-*P* clinoenstatite and clinoferrosilite (Hugh-Jones 1995), similar systematics are also likely for high-*P* clinopyroxene. The implication is that high-*P* clinopyroxene would be more disordered if equilibration at 1 atm were possible, with the greatest difference in ordering state (and K_D) is for bulk compositions lying near the middle of the join. Thus, the observed differences in Mg-Fe partitioning between high-*P* clinopyroxene, which represent the state of ordering at 9.5 GPa, and orthopyroxene, which is modeled from low pressure (mostly 1 atm) data, can be reconciled at least in part if cation ordering has a small pressure dependence. Further experimental data are required before a quantitative assessment of the pressure effect on cation ordering can be made.

Extrapolating the thermodynamic model of Kroll et al. (1997) for ordering in Mg-Fe orthopyroxene to 1275 °C yields $\Delta G^{o}_{exch} = -13.3$ kJ/mol, and when ΔG^{o}_{rec} is assumed to be equal to zero, $W^{M1} = 3.0$ kJ/mol and $W^{M2} = 1.2$ kJ/mol. These values are similar to those we derived above for the high-*P* clinopyroxene solid solutions at 1275 °C, except that the sense of asymmetry is reversed (i.e., $W^{M1} < W^{M2}$ for clinopyroxene) and that the interaction parameters have smaller values. The greater apparent non-ideality observed in the high-*P* clinopyroxenes could be an artifact of not considering a pressure effect on cation ordering when fitting the experimental data to Equation 3, because $\Delta V_{disorder}$ is a symmetric function of composition. However, the difference in asymmetry cannot be an effect of pressure.

Hazen et al. (1993) reported a $\ln K_D = 1.36$ for an orthopyroxene with $X_{Fs} = 0.44$ synthesized at 1600 °C and 11.3 GPa in a multi-anvil press. Comparison of this result with an extrapolation of the model of Kroll et al. (1997) suggests either that this orthopyroxene preserves an ordering state corresponding to ~1080 °C or that there is a significant effect of pressure on the partitioning of Fe^{2+} and Mg on the M1 and M2 sites (see Fig. 5), as was suggested by Hazen and Navrotsky (1996). It appears that high-temperature (relative to the 1 atm experiments of Anovitz et al. 1988; > 900 °C) ordering states can also be preserved in orthopyroxene when synthesized at high pressures in a multi-anvil press. In this case, partial reordering seemed to occur during the quench from 1600 °C.

In general, the state of ordering in orthopyroxene and high-*P* clinopyroxene is similar, with Fe strongly partitioned onto the M2 sites. This is consistent with the observed structural similarities between the two polymorphs. Although in detail some differences in their thermodynamic properties do exist, we conclude that orthopyroxene and high-*P* clinopyroxene have similar geochemical behavior in terms of both major and trace element partitioning. However, the thermodynamic properties of the orthorhombic to *C*2/*c* monoclinic transition itself are significant and must be considered when attempting to model the mineral assemblage of the lower upper mantle and transition zone (Woodland and Angel 1997).

Acknowledgments

The multi-anvil experiments and X-ray diffraction work were performed at the Bayerisches Geoinstitut under the EC ''Human Capital and Mobility—Access to Large Scale Facilities'' program (contract no. ERBCHGEC940053 to D.C. Rubie). Mössbauer experiments were performed with the help of equipment purchased with funds awarded to F. Seifert by Fonds der Chemischen Industrie (Germany) under the ''Materials Research'' program. N. Ross and D. Hugh-Jones are thanked for stimulating discussions during the course of this study. The thoughtful reviews of H. Kroll and H. Skogby are gratefully acknowledged.

References cited

Angel, R.J., Chopelas, A., and Ross, N. (1992) Stability of high-density clinoenstatite at upper-mantle pressures. Nature, 358, 322–324.

Angel, R.J. and Hugh-Jones, D.A. (1994) Equations of state and thermodynamic properties of enstatite pyroxenes. Journal of Geophysical Research, 99, 19777–19783.

Anovitz, L.M., Essene, E.J., and Dunham, W.R. (1988) Order-disorder experiments on orthopyroxenes: Implications for the orthopyroxene geospeedometer. American Mineralogist, 73, 1060–1073.

Canil, D. (1994) An experimental calibration of the ''nickel in garnet''

geothermometer with applications. Contributions to Mineralogy and Petrology, 117, 410–420.

Domeneghetti, M.C. and Steffen, G. (1992) M1, M2 site populations and distortion parameters in synthetic Mg-Fe orthopyroxenes from Mössbauer spectra and X-ray structure refinements. Physics and Chemistry of Minerals, 19, 298–306.

Domeneghetti, M.C., Molin, G.M., and Tazzoli, V. (1995) A crystal-chemical model for *Pbca* orthopyroxene. American Mineralogist, 80, 253–267.

Gasparik, T. (1990) A thermodynamic model for the enstatite-diopside join. American Mineralogist, 75, 1080–1091.

Ganguly, J. (1982) Mg-Fe order-disorder in ferromagnesian silicates. In S.K. Saxena, Ed., Advances in physical geochemistry, vol. 2, p. 58–99. Springer-Verlag, New York.

Hawthorne, F.C. (1988) Mössbauer Spectroscopy. In Mineralogical Society of America Reviews in Mineralogy 18, 255–340.

Hazen, R.M., Finger, L.W., and Ko, J. (1993) Effects of pressure on Mg-Fe ordering in orthopyroxene sythesised at 11.3 GPa and 1600 °C. American Mineralogist, 78, 1336–1339.

Hazen, R.M., and Navrotsky, A. (1996) Effects of pressure on order-disorder reactions. American Mineralogist, 81, 1021–1035.

Hugh-Jones, D. (1995) High pressure behaviour of pyroxenes. Ph.D. Thesis, 250 p. University of London, U.K.

Hugh-Jones, D.A., Woodland, A.B., and Angel, R.J. (1994) The structure of high-pressure *C*2/*c* ferrosilite and crystal chemistry of high-pressure *C*2/*c* pyroxenes. American Mineralogist, 79, 1032–1041.

Kroll, H., Lueder, T., Schlenz, H., Kirfel, A., and Vad, T. (1997) The Fe^{2+},Mg distribution in orthopyroxene: a critical assessment of its potential as a geospeedometer. European Journal of Mineralogy, in press.

Lindsley, D.H. (1965) Ferrosilite. Carnegie Institution of Washington Yearbook, 65, 148–149.

———(1980) Phase equilibria of pyroxenes at pressures > 1 atmosphere. In Mineralogical Society of America Reviews in Mineralogy, 7, 289–308.

McCammon, C.A., Pring, A., Keppler, H., and Sharp, T. (1995) A study of bernalite, $Fe(OH)_3$, using Mössbauer spectroscopy, optical spectroscopy and transmission electron microscopy. Physics and Chemistry of Minerals, 22, 11–20.

McCammon, C.A. and Tennant, C. (1996) High-pressure Mössbauer study of synthetic clinoferrosilite, $FeSiO_3$. In Mineral Spectroscopy: A Tribute to R.G. Burns, Geochemical Society, Special publication 5, p. 281–288.

Pacalo, R.E.G. and Gasparik, T. (1990) Reversals of the orthenstatite-clinoenstatite transition at high pressures and high temperatures. Journal of Geophysical Research, 95, 15853–15858.

Rancourt, D.G. (1989) Accurate site populations from Mössbauer spectroscopy. Nuclear Instruments and Methods in Physics Research, B44, 199–210.

Rancourt, D.G., Christie, I.A.D., Royer, M., Kodama, H., Robert, J.-L., Lalonde, A.E., and Murad, E. (1994) Determination of accurate $^{[4]}Fe^{3+}$, $^{[6]}Fe^{3+}$, and $^{[6]}Fe^{2+}$ site populations in synthetic annite by Mössbauer spectroscopy. American Mineralogist, 79, 51–62.

Rancourt, D.G. and Ping, J.Y. (1991) Voigt-based methods for arbitrary-shape static hyperfine parameter distributions in Mössbauer spectroscopy. Nuclear Instruments and Methods in Physics Research, B58, 85–97.

Sack, R.O. (1980) Some constraints on the thermodynamic mixing properties of Fe-Mg orthopyroxenes and olivines. Contributions to Mineralogy and Petrology, 71, 257–269.

Saxena, S.K. and Ghose, S. (1971) Mg^{2+}-Fe^{2+} order-disorder and the thermodynamics of the orthopyroxene crystalline solution. American Mineralogist, 56, 532–559.

Seifert, F. (1983) Mössbauer line broadening in aluminous orthopyroxenes: Evidence for next nearest neighbors interactions and short-range order. Neues Jahrbuch für Mineralogie Abhandlungen, 148, 141–162.

Shi, P., Saxena, S.K., and Sundman, B. (1992) Sublattice solid solution model and its application to orthopyroxene $(Mg,Fe)_2Si_2O_6$. Physics and Chemistry of Minerals, 18, 393–405.

Skogby, H., Annersten, H., Domeneghetti, M.C., Molin, G.M., and Tazzoli, V. (1992) Iron distribution in orthopyroxene: a comparison of Mössbauer spectroscopy and X-ray refinement results. European Journal of Mineralogy, 4, 441–452.

Sykes-Nord, J.A. and Molin, G.M. (1993) Mg-Fe order-disorder reaction in Fe-rich orthopyroxene: Structural variations and kinetics. American Mineralogist, 78, 921–931.

Thompson, J.B., Jr. (1969) Chemical reactions in crystals. American Mineralogist, 54, 341–375.

Virgo, D. and Hafner, S.S. (1969) Order-disorder in heated orthopyroxenes. Mineralogical Society of America Special Paper, 2, 67–81.

Walter, M.J., Thibault, Y., Wei, K., and Luth, R.W. (1995): Characterizing experimental pressure and temperature conditions in multi-anvil apparatus. Canadian Journal of Physics, 73, 273–286.

Woodland, A.B. and O'Neill, H.St.C. (1993) Synthesis and stability of $Fe_3^{2+}Fe_2^{3+}Si_3O_{12}$ garnet and phase relations with $Fe_3Al_2Si_3O_{12}$-$Fe_3^{2+}Fe_2^{3+}Si_3O_{12}$ solutions. American Mineralogist, 78, 1002–1015.

Woodland, A.B. and Angel, R.J. (1997) Reversal of the orthoferrosilite-high-P clinoferrosilite transition, a phase diagram for $FeSiO_3$ and implications for the mineralogy of the Earth's upper mantle. European Journal of Mineralogy, 9, 245–254.

Yang, H. and Ghose, S. (1994) In-situ Fe-Mg order-disorder studies and thermodynamic properties of orthopyroxene $(Mg,Fe)_2Si_2O_6$. American Mineralogist, 79, 633–643.

Manuscript received October 4, 1996
Manuscript accepted June 3, 1997